

MIT Open Access Articles

Amorphous InSb and InAs_{0.3}Sb_{0.7} for long wavelength infrared detection

The MIT Faculty has made this article openly available. **Please share** how this access benefits you. Your story matters.

Citation: Zens, Timothy, Piotr Becla, Anuradha M. Agarwal, Lionel C. Kimerling, and Alvin Drehman. "Amorphous InSb and InAs_{0.3}Sb_{0.7} for long wavelength infrared detection." In *Infrared Technology and Applications XXXVII*, edited by Bjørn F. Andresen, Gabor F. Fulop, and Paul R. Norton, 80123Y-80123Y-8. SPIE - International Society for Optical Engineering, 2011. © (2011) COPYRIGHT Society of Photo-Optical Instrumentation Engineers (SPIE).

As Published: <http://dx.doi.org/10.1117/12.884103>

Publisher: SPIE

Persistent URL: <http://hdl.handle.net/1721.1/79718>

Version: Final published version: final published article, as it appeared in a journal, conference proceedings, or other formally published context

Terms of Use: Article is made available in accordance with the publisher's policy and may be subject to US copyright law. Please refer to the publisher's site for terms of use.



Amorphous InSb and InAs_{0.3}Sb_{0.7} for Long Wavelength Infrared Detection

Timothy Zens, Piotr Becla, Anuradha M. Agarwal, and Lionel C. Kimerling

Microphotonics Center, Massachusetts Institute of Technology, Cambridge, MA 02139, USA

Alvin Drehman

Sensors Directorate, Air Force Research Laboratory, Hanscom Air Force Base, MA 01730, USA

Abstract

The structural, electronic, and optical properties of amorphous InSb and InAs_{0.3}Sb_{0.7} films deposited on Corning glass, Al₂O₃, CdZnTe, SiO₂-Si, and CaF₂ substrates by Radio Frequency (RF) magnetron sputtering have been studied as they relate to Mid and Long Wavelength Infrared (MWIR and LWIR) detection. Depositions at elevated substrate temperature and pressure of <10mTorr Ar show an emergence of crystalline grains with strong X-ray diffraction peaks at the (111) and (220) orientations. Electronically the amorphous InSb and InAs_{0.3}Sb_{0.7} films deposited at 300K show hopping conduction with resistance in InSb ranging from 44 to 1.1E8 Ω-cm at 300K and 84K respectively. Optical analysis using Fourier transform infrared spectroscopy (FTIR) show the absorption of these films has an absorption tail, the equation of which differing activation energies in InSb and InAs_{0.3}Sb_{0.7}. Amorphous InSb and InAs_{0.3}Sb_{0.7} films showed thermal responsivity in excess of 100V/W for 6μm thick films held at 233K. The maxima and minima of the responsivity are shown to correspond to the interference fringes in the film. The response is highly substrate dependent and compares favorably to other thermal detectors.

Keywords: InAsSb, InSb, Infrared, MWIR, LWIR, magnetron sputtering, variable range hopping

I. INTRODUCTION

Single crystal InSb and InAs_{1-x}Sb_x have been used as high mobility photodetectors in the Long Wavelength Infrared (LWIR) and Mid Wavelength Infrared (MWIR) [1,2] with detectivities approaching theoretical limits [3,4]. Sensing in the MWIR and LWIR transmission windows of the atmosphere has several applications including thermal imaging in the LWIR (8-12μm) as well as the applicability of MWIR signatures (3-8μm) for tactical guidance applications. While the quantum efficiency of HgCdTe, routinely used in IR detection, is typically higher than InAs_{1-x}Sb_x the weak Hg-Te bond makes HgCdTe much more brittle and less deployable especially for LWIR detection systems [5]. Moreover, large area HgCdTe detectors have issues with uniformity due to the high mercury vapor pressure during growth [6]. InAs_{1-x}Sb_x is of particular interest because the band gap and thus the cutoff wavelength of the detector can be tuned by changing the Sb mole fraction [7][8][9] and films at room temperature with detectivity out to 14μm have been reported [4]. However the methods used to grow these films for sensor applications, typically Molecular Beam Epitaxy (MBE) and Metal Organic Chemical Vapor Deposition (MOCVD) [4,10,11] are expensive with low throughput. These techniques also require lattice matching and/or high deposition temperatures that make monolithic integration impossible. The chemical involved with MOCVD processing are also highly toxic.

More flexible and cost effective deposition techniques such as sputtering [12] and flash evaporation [13,14] have been used to create polycrystalline and amorphous InAs_{1-x}Sb_x films. Of these two techniques sputtering offers better control of film thickness, stoichiometry, and composition for ternary systems. The structural, electronic and optical properties of these disordered systems produced by sputtering have been compared to their single crystal counterparts[15-18]. It is important to examine the effectiveness of InAs_{1-x}Sb_x detectors deposited on non lattice matched substrates at substrate

temperatures compatible with monolithic CMOS integration. This paper presents an analysis of the structural, optical, and electronic properties of both InSb and InAs_{0.3}Sb_{0.7} films deposited on Corning glass, Al₂O₃ CdZnTe, SiO₂-Si, and CaF₂ substrates. We show that amorphous InSb and InAs_{0.3}Sb_{0.7} films can be deposited using scalable techniques like RF magnetron sputtering from targets with the desired stoichiometry. The DC electrical conductivity in the temperature range of 84–340 K is measured, and a hopping conduction mechanism is identified the equation of which differs in InSb and InAs_{0.3}Sb_{0.7}. The index of refraction and extinction coefficient of the InSb films were extracted from FTIR data. X-ray diffraction (XRD) data and wavelength dispersive spectroscopy (WDS) were used to characterize the morphology and stoichiometry of the films.

II. EXPERIMENT

Films of InSb and InAs_{0.3}Sb_{0.7} varying in thickness from 100nm-7 μ m were prepared in an RF magnetron sputtering system pumped to a base pressure of 2×10^{-7} Torr by a turbomolecular pump. The gas used for sputtering was an ultra high purity Ar gas at 10mTorr. The targets were 5 cm in diameter InSb and InAs_{0.3}Sb_{0.7} disks bonded with In to a cooled copper backing plate. The polycrystalline InSb target was cast (melted, homogenized, and gradient frozen) by the Air Force Research Laboratory and was 99.999% pure with grains on the order of 3mm and the sintered 99.95% pure InAs_{0.3}Sb_{0.7} target was purchased from Plasmaterials. The substrates were optically polished CaF₂ disks from Shandong Newphotons Science and Technology Co., microscope slides from Corning glass, and oxide coated Si wafers. The Si wafers with 400 nm thermal oxide were supplied by Silicon Quest International and the Bridgeman grown Cd_{0.95}Zn_{0.05}Te substrates were supplied by the Air Force Research Laboratory. After cleaning and drying with ultra high purity nitrogen the substrates were loaded onto a resistance heating stage ($298\text{K} \leq T_{sub} \leq 775\text{K}$). The gap between the substrate and target was approximately 10 cm and the substrate was not rotated during deposition. The target was cleaned with a 30 minute presputter following which films were deposited with RF power of 50-100W at a rate of 15-25 $\text{\AA}/\text{min}$.

The structure of the films was characterized by XRD using a Philips PW1820 automatic powder diffractometer powered by a Philips PW1830 high voltage generator. The thickness of the films is measured using a Tencor P5 profilometer. A JEOL JXA-733 superprobe equipped with WDS attachment was employed for film composition analysis. Indium dots were used to form ohmic contacts onto the films for electrical conductivity and Hall measurements. The conductivity of the films at temperatures from 84 to 300 K was measured using a CTI Cryogenics 10 K refrigerator cold head model 22, a Keithley 220 programmable current source, and a Keithley 192 digital multimeter. We confirmed the ohmic nature of the contacts by the linear I-V characteristics over the temperature range. The resistance at different temperatures is extracted by least-squares linear fit of I-V curves, and the R^2 value of these fits is at least 0.95. Hall measurement is the van der Pauw technique in a magnetic field of $B=0.3\text{T}$. Substrates of CaF₂ and Cd_{0.95}Zn_{0.05}Te were chosen for their low optical absorption in the MWIR and LWIR respectively. The transmission and reflectance of these films was measured using a Perkin Elmer Spectrum 100 FTIR spectrometer. The index of refraction and extinction coefficient of the films were extracted by fitting the transmission of the films [19]. The samples were mounted on a Thermoelectric Cooler (TEC) to measure the photoresponse of the films when used as photoconductors, the samples were biased and the change in resistance of the films was measured. The signal was compared to a reference detector to obtain values for the responsivity of thin films. Films were tested at operational temperatures varying from 298 to 213K, and a Keithley 6220 current source was used to provide bias current.

III. RESULTS AND DISCUSSION

A. Structural characterization

Profilometry measurements show that the thickness of the sputtered films varies by 4-6% across a 10cm substrate. The XRD spectrum of InSb films deposited at a RF power of 100W is shown in Fig 1. When the films are deposited at substrate temperatures $<548\text{K}$ the films are amorphous and no diffraction peaks can be seen. However, for substrate temperatures $\geq 548\text{K}$ three strong peaks emerge at $2\theta= 23.8^\circ$, 39.2° and 46.4° . These peaks identify the structure as zincblende InSb (cubic, space group F43m, cell constant, $a = 6.478 \text{ \AA}$. JCPDS-PDF card number 00-006-0208 [20]).

The peak intensity ratios differ from those listed in the Powder Diffraction File (PDF) database; this is probably the result of some degree of preferential orientation.

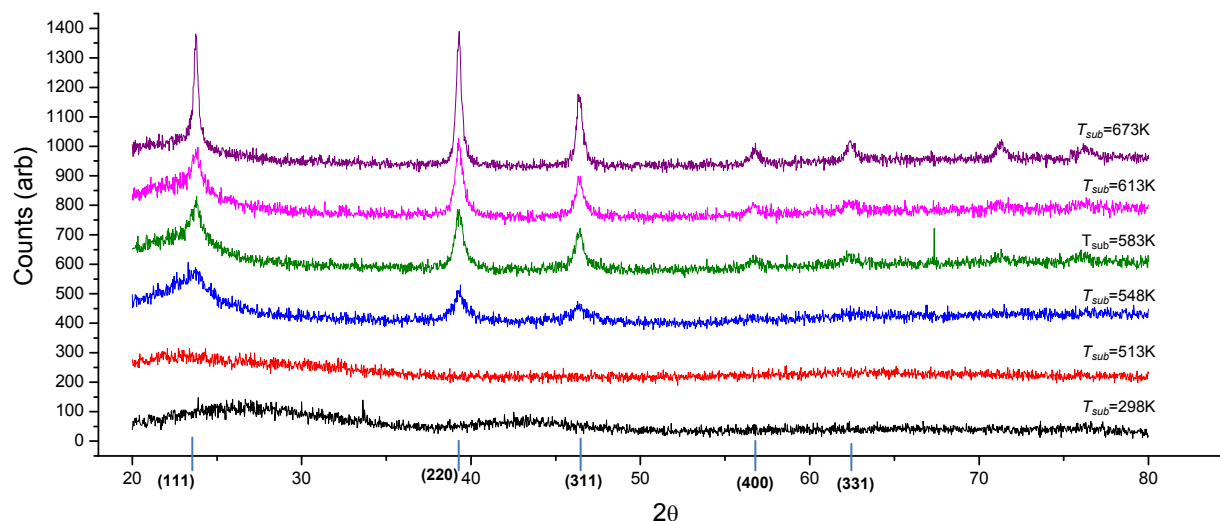


Fig 1. The XRD spectrum of InSb films sputtered onto Corning glass at various substrate temperatures. Standard XRD data of InSb powder sample [20] are also shown at the bottom for comparison. For substrate temperatures $\geq 548\text{K}$ strong peaks emerge which identify the structure as zincblende InSb. 111 and 220 orientations are the preferred film growth orientation due to lower surface energy. All samples shown are deposited on Corning glass.

The texture structure suggests that the 111 and 220 orientations are the preferred film growth orientation due to lower surface energy. This is consistent with the result of other sputtered and evaporated InSb thin films [12,21-24]. Films deposited on $\text{Cd}_{0.95}\text{Zn}_{0.05}\text{Te}$ show preferential orientation to the (111) and a larger intensity diffraction peaks at lower substrate temperatures similar to the results seen by Miyazaki *et al.* [23] when these InSb films were deposited on Al_2O_3 substrates. Table 1 shows the results of WDS on these films. Compositional analysis shows a 1:1 atomic ratio (within the error of WDS measurement 1%) for films with $T_{sub} < 613\text{K}$. However in films deposited at $T_{sub} > 613\text{K}$ we see an increase in the atomic percentage of In in the films as Sb dissociates out of the film. This phenomena was previously reported by Webb *et al.*[24].

Sample	Substrate Temperature T_{sub} (K)	Growth rate ($\text{\AA}/\text{min}$)	WDS Results	
			In at. %	Sb at. %
A	298	19.2	50	50
B	513	20.0	50	50
C	548	20.0	50	50
D	583	17.9	51	49
E	613	20.0	53	47
F	673	13.9	53	47
G	773	13.7	58	42

Table 1. WDS results for films sputtered onto heated substrates. Films with $T_{sub} < 613\text{K}$ have a 1:1 In:Sb atomic concentration, however films deposited with higher substrate temperature show an increase in the atomic percentage of In in the films and a decrease in Sb ratio consistent previous work by Webb *et al.*[24].

InAs_{0.3}Sb_{0.7} films deposited on Corning glass at $T_{sub}<673K$ were amorphous. While polycrystalline films of InAsSb have been produced by sputtering on to crystalline substrates (Al₂O₃ and GaAs) at substrate temperatures below 673K [23,25,26], no work has yet shown that these films can be deposited on amorphous substrates.

B. Electrical characterization

The amorphous InSb and InAs_{0.3}Sb_{0.7} films show very low mobility ($<1cm^2/V\cdot s$). However when InSb is sputtered onto substrates with temperatures in excess of 548K the films become increasingly n-type with higher mobility as T_{sub} increases. It should be noted that these films are deposited on glass substrates. Table 2 summarizes these results.

Sample	T_{sub} (K)	Measured at 300K			Measured at 77K		
		$\sigma(\Omega\cdot cm^{-1})$	$n(cm^3)\cdot 10^{17}$	$\mu(cm^2/V\cdot s)$	$\sigma(\Omega\cdot cm^{-1})$	$n(cm^3)\cdot 10^{17}$	$\mu(cm^2/V\cdot s)$
A	298	0.0142	-	<1	-	-	<1
B	513	0.0150	0.094	10.0	-	-	<1
C	548	1.27	1.94	41.4	0.324	1.50	14.2
D	583	15.0	5.88	159.9	8.39	4.03	129.9
E	613	16.3	6.14	165.6	9.39	4.23	138.6
F	673	24.7	7.46	206.3	13.6	5.93	141.5

Table 2. Hall results of InSb films deposited at substrate temperatures between 298 and 673K. For films deposited at substrate temperatures in excess of 548K the films become increasingly n-type with higher mobility as T_{sub} increases.

To better understand the conduction mechanisms present in the amorphous films deposited at $T_{sub}=298K$ and polycrystalline films deposited at $T_{sub}>548K$ temperature dependence of the film's dc electrical conductivity was measured and the results are shown in Fig. 2.

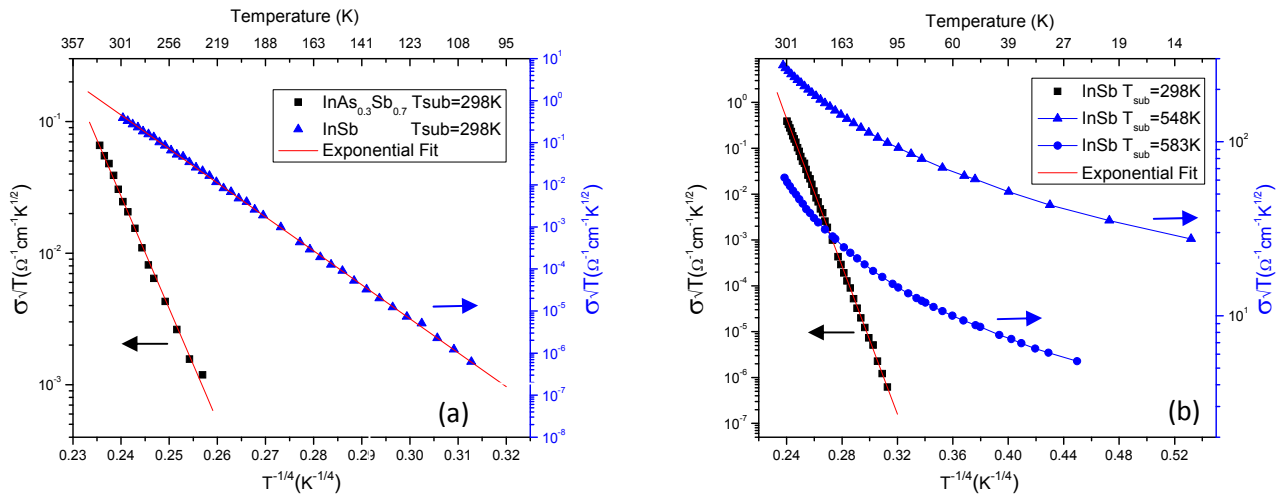


Fig 2. (a)The relation of variable range hopping in amorphous InSb and InAs_{0.3}Sb_{0.7} vs. temperature from 300 to 85K and 325K to 229K respectively. The experimentally observed behavior is in agreement with the theory laid out by Mott *et. al*. By plotting the log of the product of conductivity and the square root of temperature vs. the temperature to the inverse fourth root we can obtain a linear relation as seen. (b) A comparison conduction in InSb deposited at a substrate temperature $T_{sub}=298 K$ to that of InSb deposited at $T_{sub}=548$ and 583K. The conductivity of the films deposited at $T_{sub}\geq 548$ does not follow the $T^{-1/4}$ dependence typically seen in hopping conduction it follows an T^{-1} inverse Arrhenius law dependence.

The conductivity exhibits variable range hopping behavior. This theory laid out by Mott *et. al.* [27-29] states that the conductivity of a material is given by:

$$\sigma = \sigma_o \exp\left(-\left(\frac{T_o}{T}\right)^{1/4}\right) \quad (1)$$

Where T_o represents the strength of localization and σ_o is a constant proportional to the square root of temperature. Therefore by plotting the log of the product of conductivity and the square root of temperature vs. the temperature to the inverse fourth root we can obtain a linear relation as seen in Fig.2(a). In order for hopping transport to occur there must be a nonvanishing density of states close to the Fermi level and the Fermi level should be located within the mobility gap. The lack of nearest neighbors inherent in disordered systems often lead to localized states in the mobility gap, which contribute to hopping conduction.

Hopping conduction has previously been identified as a major electronic transport mechanism for amorphous InSb films deposited by getter sputtering at low temperatures ($T < 120\text{K}$) [15,30]. However, our films exhibit hopping conduction over a wider temperature range than previously reported results. The values of T_o are $1.1 \times 10^9\text{K}$ for InSb and $1.5 \times 10^9\text{K}$ for $\text{InAs}_{0.3}\text{Sb}_{0.7}$. These values are approximately an order of magnitude greater than the highest strength of localization reported by Hauser *et. al.* [15] for films deposited by Getter sputtering. Looking at the films deposited at $T_{sub} > 548\text{K}$ the resistivity does not follow the $T^{-1/4}$ dependence typically seen in hopping conduction it follows an inverse Arrhenius law dependence this percolation model is discussed by Gudaev *et al* [31].

C. Optical characterization

Fig.4(b) shows the measured index of refraction and extinction coefficient of the InSb film deposited at $T_{sub}=298\text{K}$ for wavelengths between 2 and $12\mu\text{m}$. The index is very close to the values for amorphous InSb found by Miyazaki *et. al.* [32]; however the absorption of the films, also shown in Fig.4, is much less than the theoretical model for evaporated films developed by Adachi *et. al.*[33]. We can fit our experimental data to an absorption band tail resulting from the disordered lattice. We fit the observed optical absorption to the equation of the absorption band tail given by:

$$\alpha \approx \exp\frac{h\nu}{E_e} \quad (2)$$

The energy E_e is a measure of structural disorder in the material. E_e is fitted from the curve slope in Fig. 3(a) giving values of 0.087 eV for InSb and 0.35 eV for $\text{InAs}_{0.3}\text{Sb}_{0.7}$. The value of E_e for InSb is very close to many nanocrystalline materials[34] however the value of $\text{InAs}_{0.3}\text{Sb}_{0.7}$ is very high indicating a high degree of disorder. Given the amorphous nature of the films the inherent disorder in structure is the cause of the absorption band tail.

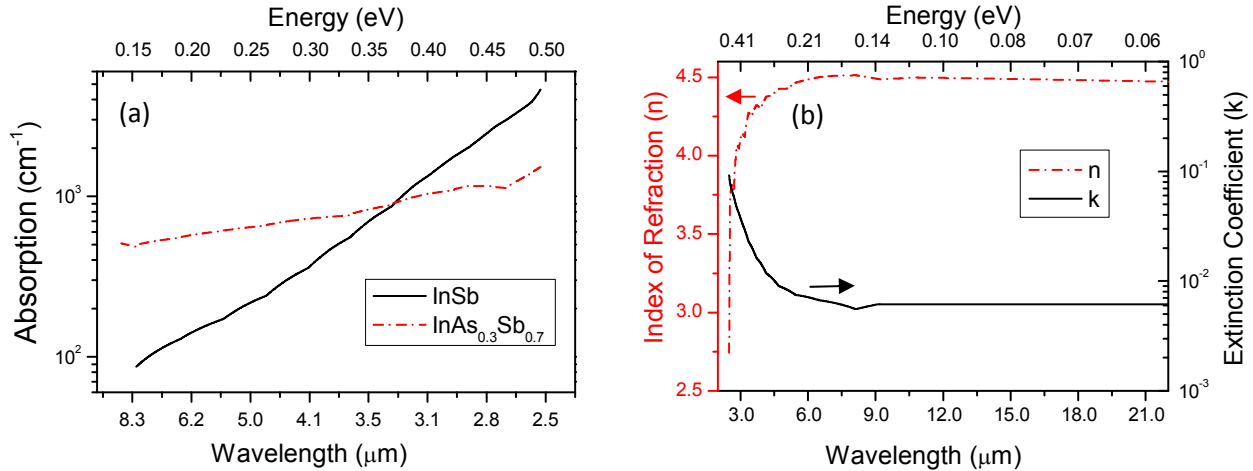


Fig 3. (a) Shows optical absorption in amorphous InSb and InAs_{0.3}Sb_{0.7} films vs. photon energy. The slope of InSb data is similar to that of many nanocrystalline materials [34] however the slope of the InAs_{0.3}Sb_{0.7} data is nearly an order of magnitude less. (b) The index of refraction and extinction coefficient of amorphous InSb vs. wavelength. The index is very close to previously reported results but the absorption is less than the theoretical model for flash evaporated films developed by Adachi *et. al.*[33].

D. Device Properties

Both the 6μm thick amorphous InAs_{0.3}Sb_{0.7} film and the 5.5μm thick amorphous InSb films showed excellent response as a thermal detector. Fig.4(a) plots the responsivity of the films with respect to the wavelength. In this graph the effects of thin film interference in the film have been removed by correlating the absorption in the film (obtained by FTIR) with the raw responsivity. Responsivities in excess of 110 and 80V/W have been obtained using the InAs_{0.3}Sb_{0.7} and InSb films respectively. The photoconductors were biased with less than 20μA current.

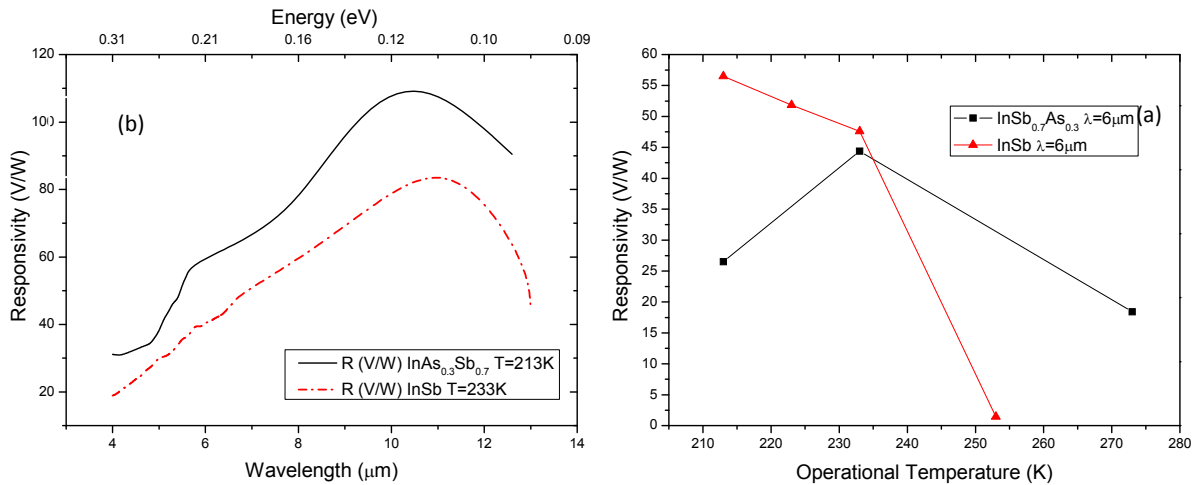


Fig 4. The responsivity of 6μm thick amorphous InAs_{0.3}Sb_{0.7} and 5.5μm thick amorphous InSb photoconductors vs. wavelength. Responsivities in excess of 110 and 80V/W have been obtained. Figure 4(b) shows the relationship of the temperature of operation to the responsivity when illuminated at 6 μm. InAs_{0.3}Sb_{0.7} films show a decrease in responsivity with when operated at temperatures cooler than 233K however the responsivity of the InSb film increases as the operational temperature is lowered to 213K.

Fig.4(b) shows the relationship between responsivity when illuminated with at 6 μm light and operational temperature in amorphous $\text{InAs}_{0.3}\text{Sb}_{0.7}$ and amorphous InSb photoconductors. The relation between responsivity and operational temperature holds true at the wavelengths between 4 and 12 μm . In the experimental set up the photoconductors are mounted onto a Thermoelectric Cooler (TEC). This TEC allows the photoconductors to operate at a range of temperatures between 298 and 213K. $\text{InAs}_{0.3}\text{Sb}_{0.7}$ films show a decrease in responsivity when operated at temperatures cooler than 233K however the responsivity of the InSb film increases as the operational temperature is lowered to 213K.

IV. Summary

In this paper, we present a systematic study on the structural, electrical, and optical properties of sputtered InSb and $\text{InAs}_{0.3}\text{Sb}_{0.7}$ films. As-deposited films are stoichiometric when deposited $T_{\text{sub}} < 548\text{K}$, zincblende polycrystals, and generally exhibit (111) texture on different substrates including amorphous glasses. We experimentally verified hopping conduction in the films at temperatures higher than 300 K. The refractive index and extinction coefficient of the films are measured at IR wavelengths. We also observe subband gap absorption due to an absorption band tail, indicating the presence of a highly disordered system.

REFERENCES

- [1] D.S.S. J.T. Wimmers, R.M. Davis, C.A. Niblack, "Indium antimonide detector technology at Cincinnati Electronics Corporation," *Proc. SPIE*, vol. 930, 1988, pp. 125-138.
- [2] D.S.S. J.T. Wimmers, "Characteristics of InSb photovoltaic detectors at 77 K and below," *Proc. SPIE*, vol. 364, 1983, pp. 123-131.
- [3] J. Altmann, S. Kohler, and W. Lahmann, "Fast current amplifier for background-limited operation of photovoltaic InSb detectors," *Journal of Physics E*, vol. 1275, 1980.
- [4] A.M.R. J. D. Kim, S. Kim, D. Wu, J. Wojkowski, J. Xu, J. Piotrowski, E. Bigan, "8–13 μm InAsSb heterojunction photodiode operating at near room temperature," *Appl. Phys. Lett.*, vol. 67, Oct. 1995, pp. 2645-47.
- [5] T. Niedziela and R. Ciupa, "Ultimate parameters of $\text{Hg}_{1-x}\text{Cd}_x\text{Te}$ and $\text{InAs}_{1-x}\text{Sb}_x$ n \square p photodiodes," *Solid-State Electronics*, vol. 45, 2001, pp. 41-46.
- [6] A. Rogalski, "Infrared detectors: an overview," *Infrared Physics & Technology*, vol. 43, Jun. 2002, pp. 187-210.
- [7] W. Coderre John, "Electrical Properties on $\text{InAs}_x\text{Sb}_{(1-x)}$ alloys," *Canadian Journal of Physics*, vol. 46, 1968, pp. 1207-1214.
- [8] J.C. Woolley and J. Warner, "OPTICAL ENERGY-GAP VARIATION IN InAs-InSb ," *Canadian Journal of Physics*, vol. 42, 1964, pp. 1879-1887.
- [9] and A.Y.C. M. Y. Yen, R. Peopie, K. W. Wecht, "long-wavelength Photoluminescence of $\text{InAs}_{1-x}\text{Sb}_x$ ($0 < x < 1$) grown by molecular beam epitaxy on (100) InAs," *Appl. Phys. Lett.*, vol. 52, 1987, pp. 489-491.
- [10] P.K. Chiang and S.M. Bedair, "p-n junction formation in $\sim\text{nSb}$ and $\text{InAs}_{1-x}\text{Sb}_x$ by metalorganic chemical vapor deposition," *Applied Physics Letters*, vol. 46, 1985, pp. 383-385.
- [11] J.B. Cohen, J. Carsello, V.P. Dravid, C. Besikci, Y.H. Choi, G. Labeyrie, E. Bigan, and M. Razeghi, "Detailed analysis of carrier substrates by metalorganic ort in $\text{InAs}_{0.3}\text{Sb}_{0.7}$, layers grown on GaAs substrates by metalorganic chemical-vapor deposition," vol. 76, 1994.
- [12] J.E. Greene and C.E. Wickersham, "Structural and electrical characteristics of InSb thin films grown by rf sputtering," *Journal of Applied Physics*, vol. 47, 1976, p. 3630.
- [13] VH, "Electrical Properties of Annealed InSb Thin Films," *physica status solidi* (, vol. 81, 1984, p. K195-K197.

- [14] M, "Dendritic crystal regrowth and electrical properties of InSb thin films prepared by vacuum evaporation," *Journal of Applied Physics*, vol. 66, 1989, pp. 4252-4257.
- [15] J.J. Hauser, "Electrical Properties of Amorphous InSb," *Physical Review B*, vol. 8, 1973, pp. 2678-2684.
- [16] T. Miyazaki and S. Adachi, "Optical properties of InSb films deposited on sapphire substrates by rf sputtering," *Journal of Applied Physics*, vol. 70, 1991, pp. 1672-1677.
- [17] P. Scholte, "Crystallization kinetics of thin amorphous InSb films," *Materials Science and Engineering: B*, vol. 5, 1990, pp. 233-237.
- [18] T.S. Rao, C. Halpin, and J.B. Webb, "Effect of substrate temperature on the growth rate and surface morphology of heteroepitaxial indium antimonide layers grown on (100) GaAs by metalorganic magnetron sputtering," vol. 65, 1989, pp. 585-590.
- [19] M. Mulato, I. Chambouleyron, E.G. Birgin, and J.M. Martínez, "Determination of thickness and optical constants of amorphous silicon films from transmittance data," *Applied Physics Letters*, vol. 77, 2000, p. 2133.
- [20] H.E. Swanson, R.K. Fuyat, and G. Ugrinic, *National Bureau of Standards Circular*, 1955.
- [21] I. Khan, "Epitaxial growth of indium antimonide films as studied in situ by electron diffraction," *Surface Science*, vol. 9, 1968, p. 306-324.
- [22] J. Červenák, A. Živčáková, and J. Buch, "Structure and electrical properties of InSb thin films prepared by plasmatic sputtering," *Czechoslovak Journal of Physics*, vol. 20, 1970, p. 84-93.
- [23] T. Miyazaki, M. Mori, and S. Adachi, "Epitaxial growth of InSb on sapphire by rf sputtering," *Applied Physics Letters*, vol. 58, 1991, pp. 116-118.
- [24] J. Webb, C. Halpin, J. Ehrismann, and J. Noad, "The preparation of epitaxial InSb films by magnetron sputtering," *Canadian Journal of Physics*, vol. 65, 1987, p. 872-877.
- [25] C. Peng, N. Chen, J. Wu, Z. Yin, and Y. Yu, "Magnetron sputtering growth of InAs_{0.3}Sb_{0.7} films on (1 0 0) GaAs substrates: Strong effect of growth conditions on film structure," *Journal of Crystal Growth*, vol. 285, 2005, pp. 459-465.
- [26] T. Miyazaki, M. Kunugi, Y. Kitamura, and S. Adachi, "Epitaxial growth of InSb films by rf magnetron sputtering," *Thin Solid Films*, vol. 287, 1996, pp. 51-56.
- [27] N.F. Mott, "Conduction in non-crystalline systems," *Philosophical Magazine*, vol. 24, Jul. 1971, pp. 1-18.
- [28] A. Lewis, "Evidence for the Mott model of hopping conduction in the anneal stable state of amorphous silicon," *Physical Review Letters*, vol. 29, 1972, p. 1555.
- [29] A.Y. Rogatchev and U. Mizutani, "Hopping conductivity and specific heat in insulating amorphous TixSi100-x alloys," *Physical Review B*, vol. 61, Jun. 2000, pp. 15550-15553.
- [30] H. Theuerer and J. Hauser, "Getter Sputtering for the Preparation of Thin Films of Superconducting Elements and Compounds," *Journal of Applied Physics*, vol. 35, 1964.
- [31] O. Gudaev, V. Malinovsky, E. Paul, and V. Treshikhin, "Nonactivation nature of conductivity in disordered materials," *Solid State Communications*, vol. 74, 1990, p. 1169-1173.
- [32] S. Adachi, "Optical dispersion relations in amorphous semiconductors," *Physical review. B, Condensed matter*, vol. 43, May. 1991, pp. 12316-12321.
- [33] T. Miyazaki and S. Adachi, "Analysis of Optical Constants for Sputter-Deposited InSb Films Based on the Interband-Transition Model," *Jpn. J. Appl. Phys. Vol.*, 1992.
- [34] J. Tauc, *Amorphous and Liquid Semiconductors*, 1974.